Effects of Collisions on Saturation Behavior of the 1.15-μ Transition of Ne Studied with He-Ne Laser*

A. Szöke† and A. Javan
Physics Department, Massachusetts Institute of Technology, Cambridge, Massachusetts
(Received 28 June 1965; revised manuscript received 16 December 1965)

The frequency response of the output power of a single-mode He-Ne gas laser has been studied in detail. This has been done in order to obtain information on the effects of atomic collisions on the frequency response of the individual atoms. At the operating pressures, the collision widths were considerably smaller than the Doppler width. From these measurements we find that in addition to pressure-dependent broadening due to hard collisions, there exists appreciable broadening due to soft collisions. Furthermore, we find the atomic collisions lead to an asymmetry in the average frequency response of individual atoms. It is shown that this slight asymmetry of the atomic response leads to a sizable shift of the frequency of the minimum of the Lamb dip where the effect of saturation is maximum. This shift has been obtained and is found to be pressure-dependent.

1. INTRODUCTION

GASEOUS lasers (optical masers) make a powerful tool in spectroscopy by providing a coherent, monochromatic light source of high intensity. Thus, many of the techniques of microwave spectroscopy can be transferred to the optical region of the spectrum. In this paper some measurements are reported concerning the behavior of the output power of a He-Ne gas laser. The work is a continuation of that reported in previous letters.[1,2]

Just as the ammonia maser provides information on the spectrum of ammonia itself, the He-Ne gas laser may be used to obtain spectroscopic information about the line shape and pressure broadening of the 1.15-μ transition of Ne responsible for laser action, $2p^5(^2P_{1/2}{}^0)4s(J=1) \rightarrow 2p^5(^2P_{1/2}{}^0)3p(J=2)$. The method used is to measure the output power of a gas laser as a function of its frequency while the laser is operated in a single longitudinal mode (single-cavity resonance) and its frequency is tuned by changing the distance between the mirrors comprising the cavity.

As the frequency approaches that of the peak of the atomic transition (atomic resonance), the gain of the medium increases and the output power may be expected to rise. However, it has been predicted by Lamb[3] that in a gas, at short wavelengths, the power output of the laser is limited by saturation to a value which is smaller at resonance than on either side of it. The frequency interval of the "power dip" where the excess saturation occurs is of the order of the atomic linewidth, inclusive of pressure broadening, but not including Doppler broadening. This power dip was initially observed by the authors[2] and by McFarlane, Bennett, and Lamb.[4] Details of the atomic line shape are manifested in the exact shape of the dip and can be inferred by numerical analysis of it. Experiments have been repeated at several different gas pressures; this way collision cross sections have been obtained.

In order to get this information, Lamb's theory of the optical maser[3] must be generalized to include arbitrary line shapes and effects of distant atomic collisions causing an "inhomogeneous" line broadening. A restatement of Lamb's theory in simple terms will be given,[5] and a generalization to include the above effect offered.

2. EXPERIMENTAL

Figure 1 is a block diagram of the apparatus. A He-Ne laser of sturdy construction was used. It had internal plane mirrors coated for high reflectivity at the 1.15-μ transition of neon. The discharge was maintained by a radio-frequency transmitter delivering approximately 30 W at a 14-Mc/sec frequency. The mirror separation was about 50 cm and could be changed slightly by sending current through coils wrapped around four Invar spacers, thereby causing magneto-

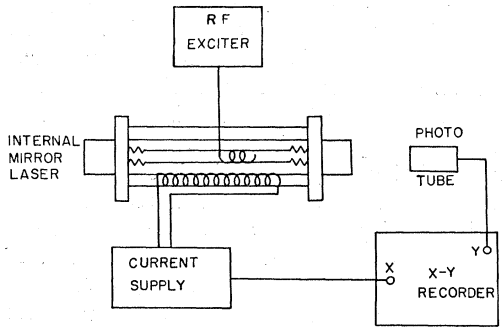

FIG. 1. Block diagram of the apparatus for measurement of the power output of a gas laser as a function of its frequency.

* Work supported by the National Aeronautics and Space Administration and Air Force Cambridge Research Laboratories.
† Present address: Weizmann Institute, Rehovoth, Israel.
[1] A. Szöke and A. Javan, Phys. Rev. Letters **10**, 521 (1963).
[2] A. Szöke, Bull. Am. Phys. Soc. **9**, 65 (1964).
[3] W. E. Lamb, Phys. Rev. **134**, A1429 (1964).
[4] R. A. McFarlane, W. R. Bennett, and W. E. Lamb, Appl. Phys. Letters **2**, 189 (1963).
[5] Notwithstanding the warning issued in Lamb's paper [Ref. 3, p. A1448, Sec. 18].

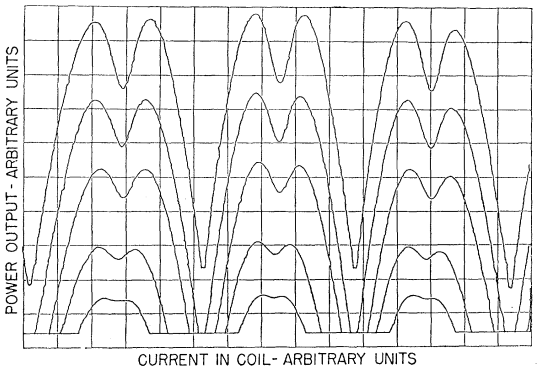

FIG. 2. Actual recording of power output of a gas laser as a function of cavity length. The multitude of traces is explained in the text.

striction.[6] In order to ensure stability of the laser frequency over a period of a few minutes while the data were taken, it was important to insulate the laser acoustically and thermally from its surroundings. This was achieved by putting the laser on a heavy table which was placed on top of inflated airplane inner tubes. The table had a resonant frequency of approximately 5 cps. The room was temperature controlled and magnetostrictive currents, as well as the excitation of the plasma, were kept as constant as possible. The laser was filled and sealed off to a relatively high initial pressure at the desired composition of He and Ne^{22}. Enriched Ne^{22} isotope was used throughout this work. In order to change the pressure of the active gas while maintaining its composition, evacuated bottles of known volume were attached to the active volume of the laser via break seals. This allowed changing the volume of the gas in several steps after each filling of the laser. The initial gas pressures were measured with a membrane manometer during filling of the lasers and were accurate to about 10%. Greater accuracy in gas pressure measurement would involve taking samples of the gas during the actual running of the experiment since there is penetration of the gas into the walls. (After a full pumpdown cycle, including baking of the tube, as much as 2% of the previous neon content still remained!)

The ouptut power of the laser was measured using an RCA 7102 multiplier phototube without any attenuation and was displayed on the Y axis of an X-Y recorder. The X axis was proportional to the current across the magnetostrictive coil, and so, indirectly, the frequency of the maser was recorded on a recurrent scale as successive cavity resonances entered the frequency region of high gain of the Doppler-broadened transition. An actual recording is reproduced in Fig. 2.

The laser was operated in a single longitudinal mode of the cavity and all transverse modes were eliminated. This was achieved by accurate alignment of the mirrors, low excitation powers, and short discharges. There was indirect evidence of single-mode operation since the laser, when tuned, stopped oscillating between intensity maxima. The absence of irregularities of any kind in the data, and their excellent fit to the theoretical expressions, also confirm single-mode oscillation.

Care was taken to eliminate the Zeeman effect due to the earth's or stray magnetic fields by providing μ-metal shields surrounding the discharge tube. The output of the laser was linearly polarized. The direction of polarization remained entirely fixed throughout the range of laser tuning.

In order to study the inherent asymmetry of the neon line shape, some sources of spurious asymmetry were carefully eliminated. The isotope Ne^{22} was chosen, because the presence of Ne^{20} in the gas mixture would cause an asymmetry opposite to the one observed experimentally. For this very reason the results on asymmetry are lower limits. Also, it can be estimated that spurious resonances within the interferometer mirrors or coating themselves can cause asymmetries which are smaller by at least an order of magnitude than the observed values. Moreover, these asymmetries were obtained with at least two different sets of mirrors, which tend to rule out any accidental coincidence in this direction.

3. ANALYSIS OF MEASUREMENTS

Results were analyzed on a digital computer. Curves similar to those in Fig. 2 were fitted to a theoretical formula containing five free parameters. This theoretical formula, the outline of the calculation, and various experimental correction factors are presented in this section.

In Fig. 2 there are many tracings of various heights, corresponding to different discharge intensities. Laterally, each tracing is made up of three repetitions. These arise from three consecutive modes of the Fabry-Perot cavity characterized by $2L/\lambda = n+1, n+2$; where L is the cavity length, λ the wavelength of the light, and n is of the order of 10^6. This repetition calibrates the X axis in terms of frequency, the spacing between modes being known. As the length of the laser increases, the frequency of oscillation of a given mode decreases until the next mode has higher gain and begins to oscillate. Then the laser frequency jumps to its highest value (in single-mode operation) and as the length continues to change, the frequency starts to decrease again. Only the central mode was analyzed; the two others served as checks and were also used to correct slight distortions due to the apparatus. It was important to eliminate these distortions in order to arrive at valid parameters, especially in measuring asymmetric line shapes.[7]

There are two experimental imperfections for which corrections have to be made, both connected with the magnetostrictive tuning technique. The X axis of

[6] W. R. Bennett and P. J. Kindlmann, Rev. Sci. Instr. 33, 601 (1962).

[7] K. Shimoda and A. Javan, J. Appl. Phys. 36, 718 (1965).

Fig. 2 is proportional to the current in the coils, and hence to the H field which causes magnetostriction. Unfortunately, the length of the spacers does not depend linearly on this H field; rather it follows an S-shaped curve. All experiments were done on the straightest portion of this curve. The remaining nonlinearity in the frequency scale was corrected for in the numerical analysis by fitting a third-order polynomial to four well-defined points $KLMN$ in Fig. 3. The linear part of the scale was obtained by noting that the distance in frequency between two adjacent modes is $c/2L$. Frequency pulling is not taken into account, as it is always smaller than other experimental errors. The third-order correction turned out to be small.

For actual analysis of the data the frequency on the X scale is needed in units of the Doppler linewidth $\Delta\omega$ [see Eq. (18)]. It was assumed that $\sqrt{2}\Delta\omega = 450$ Mc/sec, as theoretical analysis showed the frequency dependence of the output power of a laser operating slightly above threshold is insensitive to the exact value of the Doppler linewidth.

Another small but significant correction stemmed from the fact that we were unable to keep the mirrors exactly parallel while changing the distance between them. About 1 sec of arc misalignment gives a significant increase in the losses of the cavity and thus a decrease in the output power of the laser. It should be pointed out that we were able to reduce the actual deviations from parallel movement to a very small amount. The remaining influence of this mirror tilt was corrected from our final data. This correction was assumed to be a quadratic function of the sweep current. The constants of the quadratic were determined from points OPQ on Fig. 3. All told, five experimental parameters were used to account for the various distortions along the coordinate axes. These were manually computed as described above—the distortions of the X scale for each page of graph (e.g., the whole of Fig. 2) and the distortion of the Y scale for every trace on a graph. There were about 80 traces analyzed in the whole experiment.

According to the theory expounded in Sec. 4 of this paper Eq. (45) was used to fit experimental data. This equation is reproduced here in the form it was actually used after the removal of all experimental distortions.

$$Y = A[B - \exp(x^2)] \Big/ \left[1 + \frac{C^2 D}{C^2 + (x-E)^2}\right]. \quad (45a)$$

Ordinates from the center portion of each trace were read off in arbitrary units, one for each small division on the X scale, and were fed into the computer. The computer program fitted experimental data with five *free* parameters, $ABCDE$, calculated the mean-square error, and tried to reduce that error by choosing better parameters. As the equation is nonlinear, an iterative procedure was adopted. As a function of the five free parameters, the mean-square error determines a surface

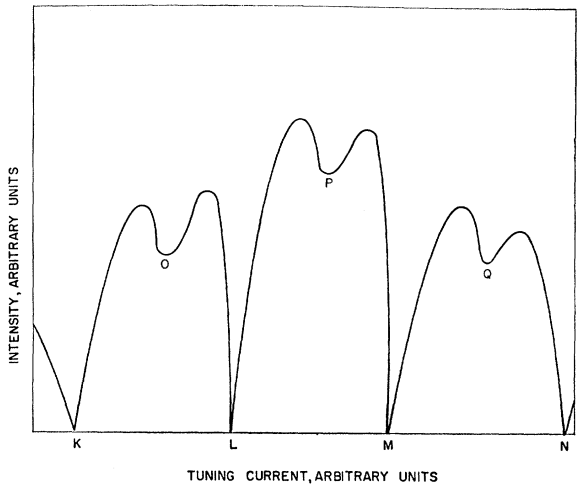

FIG. 3. Schematic representation of a trace of Fig. 2, at a single excitation level, in order to demonstrate the way the distortions were rectified. Distortions shown are exaggerated.

in six-dimensional space. Starting at an arbitrary point, the direction of the gradient of the surface was found. Two steps of a predetermined magnitude were taken along the gradient, and a parabolic extrapolation was made to find the minimum in this direction. At the newly found point the procedure was repeated. Results were considered satisfactory if the new values of the parameters were within a prescribed small distance from their previous values. This program proved to be very efficient, probably because of the general smoothness of the surface. Usually a standard deviation of 1% of $Y_{\max}$ was considered satisfactory. The fit was so close that it is impossible to distinguish between experimental and fitted curves on the scale of a *Physical Review* page.

It should be stressed that the results do not in themselves check the validity of the *form* of Eq. (45a). The experiment confirms only that a family of curves can be fitted with essentially the same values of A, B, C, D, E, and it is used to obtain their numerical values.

4. THEORY

A. Simplest Version

In this section, a simplified theory of the operation of a gas laser will be given. In spite of its limitations and the existence of a more fundamental theory,[3] this model is given here because of its simiplicity; it emphasizes some of the physical assumptions and limitations common to all existing theories. In particular, this formulation will allow the effects of collisions between atoms to be included with fair ease.

Consider a gas consisting of a collection of atoms in thermal motion influenced by an electromagnetic plane-wave field. It is assumed that this electromagnetic field has a frequency ω near that of one of the atomic transitions ω_0 so that all other atomic transitions can be ignored. The atoms will be characterized by their

populations in these two states of interest $n_1(v)$, $n_2(v)$, where v denotes the component of the atomic velocity along the axis of propagation of the field. The quantities $n_1(v)$, $n_2(v)$ denote populations per unit volume per unit velocity. It is the difference between these numbers, $n(v)=n_1(v)-n_2(v)$, which enters the simplified theory. It is stipulated that for an inverted population, $n(v)>0$. Only stimulated emission will be taken into account, and even that in its simplest form. Thus the intensity I, emitted per unit length by the gas atoms under the influence of a traveling electromagnetic field wave vector k and frequency ω, is

$$\frac{dI(k,\omega)}{dx}=\frac{c}{8\pi}\int n(v)\sigma(v,k,\omega)E^2(k,\omega)\,dv, \tag{1}$$

where $\sigma(v,k,\omega)$ is a cross section for emission of light by an atom with velocity component v and stimulated by an electromagnetic wave with frequency ω and wave vector k. Specifically, $\sigma(v,k,\omega)$ represents an ensemble average of the response of those atoms which have velocity v. This ensemble average may already include certain pressure effects to be described later.

In case the applied electromagnetic wave is of a more general nature than a simple traveling wave, Eq. (1) may still be applied after the wave is expanded into traveling wave components and written in the form

$$E=\sum_{k,\omega} E(k,\omega)\cos(kx-\omega t). \tag{2}$$

The general form of the response function including the Doppler effect is

$$\sigma(v,k,\omega)=F\{\omega_0-\omega[1+(\mathbf{k}\cdot\mathbf{v}/|\mathbf{k}|c)]\},$$

F being an arbitrary function, peaked around ω_0. In order to be more specific, at some points a Lorentz line shape is assumed,

$$\sigma(v,k,\omega)=\sigma_0\Big/\left\{1+\left[\omega-\omega_0\left(1-\frac{\mathbf{k}\cdot\mathbf{v}}{|\mathbf{k}|c}\right)\right]^2 T_2^2\right\}, \tag{3}$$

where T_2^{-1} is the half-width of the resonance in radians and

$$\sigma_0=8\pi^2\mu^2T_2/h. \tag{4}$$

The transition is assumed of electric dipole type of moment μ. Note that the Doppler effect in (3) is written in a form giving an appearance of a shift of the resonance frequency of the atom. This form is very closely related to that used in the above expression for F where the shift is introduced on the frequency of the applied field.

The above approach to calculating the nature of emitted light from a cross section is certainly valid if the atoms are moving in a straight line with constant velocity during their time of coherent interaction with the electromagnetic field, i.e., for low pressures and moderately high electric fields. Actually, it also has more general validity, as will be seen in greater detail in the next section.

In a maser oscillator, $E(\omega)$ and $n(v)$ have to satisfy two equations. One is the expression for the energy balance of the cavity. The other one is a Boltzmann equation for the energy balance of the atomic system. First, it is noticed that if there is population inversion, the medium has an exponential gain $G(k,\omega)$ for a traveling electromagnetic wave of intensity I, having the proper frequency. It is given by

$$G(k,\omega)=\frac{d\ln I}{dx}=\int n(v)\sigma(v,k,\omega)\,dv. \tag{5}$$

In steady state, the total gain equals the total loss. While the gain is distributed within the medium, the loss is usually concentrated at the ends of the laser. Though it is easy to write down the requisite equation, it is simpler to assume an "equivalent" loss per unit length L. In a steady state this implies that the electromagnetic field is constant over the length of the tube. Thus the discussion is limited to lasers with small end losses: mirrors of high reflectivity, and low diffraction. Thus, the equation describing the energy balance may be written as

$$L=G(k,\omega)=\int n(v)\sigma(v,k,\omega)\,dv. \tag{6}$$

In a laser oscillator, the optical frequency field is essentially at the resonance frequency of the cavity (see Appendix). Because of the saturation effect, $n(v)$ is dependent on E^2. Once this dependence is known, (6) may be used to obtain the laser output.

The energy balance for the atomic system is given by the Boltzmann equation. In steady state this is

$$0=\frac{dn(v)}{dt}=\left(\frac{\partial n(v)}{\partial t}\right)_{\text{collisions}}-\frac{n(v)}{T_1}-\sum_{k,\omega}\frac{2}{h\omega}n(v)\sigma(v,k,\omega)E^2(k,\omega)\frac{c}{8\pi}. \tag{7}$$

The first term on the right-hand side is the collision term. Two different types of collisions can be distinguished: inelastic collisions in which the total population difference changes and elastic collisions which involve only a change in velocity. The former includes processes which populate or deplete the levels in question, like pumping light or atomic and electron impacts. The latter type are those collisions in which the number of atoms in each atomic-energy level remains unchanged; however, the collisions lead to changes in velocity of the colliding atoms. The third term describes the influence of stimulated emission.

In the absence of an applied electromagnetic wave, the velocity distribution of atoms in an excited state will become Maxwellian if the excited atoms suffer a

number of elastic collisions within their lifetimes. For atoms in the $2s_2$ level of Ne, the velocity distribution may be somewhat different from Maxwellian. However, as long as the velocity distribution is such that the resulting Doppler width is appreciably larger than the natural or collision width of the atoms, the exact form of the velocity distribution is not of major importance in our consideration. Accordingly, we assume that in the absence of the optical maser field, the velocity distribution of the population difference $n_0(v)$ is given by

$$n_0(v)=[n/u(2\pi)^{1/2}]\exp(-v^2/2u^2), \tag{8}$$

where $u^2=kT/m$ with k as the Boltzmann constant, T as the temperature, and m, the atomic mass. Thus to this approximation,

$$0=[\partial n_0(v)/\partial t]_{\text{collisions}}-[n_0(v)/T_1]. \tag{9}$$

In the presence of the laser field, the change in the collision rate may be written as

$$[\partial n(v)/\partial t]_{\text{collisions}}-[\partial n_0(v)/\partial t]_{\text{collisions}} =-[n(v)-n_0(v)]pW_c, \tag{10}$$

where pW_c is a "cross relaxation" rate, proportional to the pressure p of the gas. It should be noted that the underlying assumption leading to (10) is the fact that the rate of approach of the velocity distribution to thermal equilibrium is taken independent of velocity and an exponential approach to the equilibrium is assumed. In an actual case, this assumption may not hold over a large range of velocity. However, using (10) a great deal of simplification will result.

Subtraction of (9) from (7) and substitution from (10) yields:

$$0=-\frac{n(v)-n_0(v)}{T_1'}-\sum_{k,\omega}\frac{2}{h\omega}n(v)\sigma(v,k,\omega)E^2(k,\omega)\frac{c}{8\pi}. \tag{11}$$

Here $(T_1')^{-1}=T_1^{-1}+pW_c$ is a total relaxation rate in the presence of laser action.

At this point Eqs. (6) and (11) can be solved for $n(v)$ and $E^2(k,\omega)$ which may then be used to estimate the laser output power.

The solution of Eqs. (6) and (11) will now be worked out for a traveling-wave laser and for a standing-wave laser, both operating on a single frequency. For a traveling-wave laser Eqs. (2), (6), and (11) take the following simple form:

$$E=E(k,\omega)\cos(kx-\omega t),$$

$$L(k,\omega)=\int n(v)\sigma(v,k,\omega)\,dv, \tag{12}$$

$$n(v)=n_0(v)[1+T_1'E^2\sigma(v,k,\omega)]^{-1} \approx n_0(v)[1-T_1'E^2\sigma(v,k,\omega)].$$

Substitution yields

$$L=\int n_0(v)\sigma(v,k,\omega)\,dv -T_1'E^2(k,\omega)\int n_0(v)\sigma^2(v,k,\omega)\,dv. \tag{13}$$

The operating frequency of the laser is determined by the phase equation, discussed in the Appendix. For most practical cases it is near the frequency of the unloaded cavity. The first term on the right-hand side is the gain of the medium in the absence of the output power. The second term is negative and it describes the decrease in gain as a consequence of depletion of the upper maser level, i.e., a decrease in population inversion caused by the electromagnetic field. The frequency dependence of this equation can be evaluated easily if Doppler broadening exceeds the atomic linewidth: $T_2^{-1}\ll ku$. Then $n_0(v)$ is a slowly varying function compared to either σ or σ^2 and it can be replaced by its value at the peak of σ,

$$n_0(v)=\frac{n}{u(2\pi)^{1/2}}\exp\left[-\frac{(\omega-\omega_0)^2}{2\Delta\omega^2}\right], \tag{14}$$

where

$$\Delta\omega=\omega_0(u/c).$$

It is useful to introduce the notation:

$$G_0(k,\omega)\approx G_0\exp[-(\omega-\omega_0)^2/2\Delta\omega^2],$$

$$G_0=\frac{n}{u(2\pi)^{1/2}}\int\sigma(v,k,\omega_0)\,dv. \tag{15}$$

Finally the laser output is

$$I\approx\frac{c}{8\pi}(1-R)AE^2(k,\omega)\approx\left(\frac{c}{8\pi}\right)\frac{(1-R)A}{T_1'\int\sigma^2(v,k,\omega_0)\,dv} \times\left\{G_0-L\exp\left[+\frac{(\omega-\omega_0)^2}{2\Delta\omega^2}\right]\right\}, \tag{16}$$

where $(1-R)$ denotes the transmission of the mirrors, and A is the effective area of the emerging beam. This result can be compared to the exact calculation[8] for the saturated laser. A positive exponential appears in the frequency dependence of the output power, and thus the power falls to zero with an ever increasing slope as the cavity is detuned. The maximum frequency range of oscillation in a high-gain gas laser gives a good

[8] There is an apparent discrepancy in the exponential which stems from an approximation made in Ref. 3. The integration in Eq. (71) of Ref. 3 can be carried out even if $\exp[-1/4(ku)^2\times(\tau'''-\tau')^2]$ is not substituted by a delta function, and the result is identical to ours.

indication of the gas kinetic temperature of the excited state.

A standing-wave laser emitting a single frequency will be treated next. The electromagnetic field can be decomposed into two running waves propagating in opposite directions:

$$E=E(k,\omega)\cos(kx-\omega t)+E(-k,\omega)\cos(-kx-\omega t),\quad E(k,\omega)=E(-k,\omega). \tag{17}$$

In place of Eq. (6) we write

$$L=\int n(v)[\sigma(v,k,\omega)+\sigma(v,-k,\omega)]\,dv. \tag{18}$$

This is more accurate than Eq. (6), as it takes into account the fact that losses as well as gain are associated with cavity modes, and these in turn have been decomposed into running waves. For more details see the Appendix. Equation (11) is written next and solved:

$$n(v)=n_0(v)\frac{1}{1+T_1'E^2(k,\omega)[\sigma(v,k,\omega)+\sigma(v,-k,\omega)]}$$
$$\approx n_0(v)\{1-T_1'E^2(k,\omega)[\sigma(v,k,\omega)+\sigma(v,-k,\omega)]\}. \tag{19}$$

Analogously to the running-wave case, Eq. (18) gives

$$L=\int n_0(v)[\sigma(v,k,\omega)+\sigma(v,-k,\omega)]\,dv - T_1'E^2(k,\omega)\int n_0(v)[\sigma(v,k,\omega)+\sigma(v,-k,\omega)]^2\,dv. \tag{20}$$

The first term on the right can again be identified as the unsaturated gain, and denoted by $G_0(\omega)$. The second term is negative and it describes the saturation. The coefficient of E^2 is an effective coupling between the light and the inverted population. Its frequency dependence is evaluated next for a line with strong Doppler broadening and a Lorentzian line shape:

$$\int n_0(v)[\sigma(v,k,\omega)+\sigma(v,-k,\omega)]^2\,dv \approx n_0(v_0)\frac{c\pi\sigma_0^2}{\omega_0 T_2}\left[1+\frac{1}{1+(\omega-\omega_0)^2T_2^2}\right]. \tag{21}$$

The first term of the result is similar to the running-wave case, but the second term shows an additional feature. If the frequency of the electromagnetic field is near that of the atomic resonance, some of the atoms emit into both running-wave components; thus they are acted upon by a larger effective field or, equivalently, E has a larger coupling to the population. Finally the laser output power is obtained:

$$I(\omega)\approx(c/8\pi)(1-R)AE^2(k,\omega) \approx\frac{c}{4\pi}\frac{(1-R)Au(2\pi)^{1/2}\omega_0T_2}{2T_1'c\pi\sigma_0^2n} \times\left(\frac{G_0-L\exp[+(\omega-\omega_0)^2/2\Delta\omega^2]}{1+[1+(\omega-\omega_0)^2T_2^2]^{-1}}\right). \tag{22}$$

This equation shows the dip; in fact it is completely equivalent to Lamb's Eq. (96).[3]

In the Appendix it will be shown that by taking the proper phase angle in σ, the frequency part of the laser equations can also be obtained correctly. Our treatment is completely equivalent to Lamb's to the second order.

B. Pressure Broadening

The stimulated emission cross section $\sigma(v,k,\omega)$ has been introduced so far as a phenomenological parameter. In this section an attempt will be made to clarify its shape in terms of the physical processes involved, natural decay (radiative and nonradiative) and collisions of the radiating atom. It will also be shown that certain aspects of the atomic collisions are not properly accounted for in the theory as presented so far, namely the influence of collisions of large impact parameter, when the radiating atom is deviating but little from its original course. Some approximate ways of doing this will be shown, and the theory will be compared to experiment in the last chapter of this paper.

It is clear from the outset that a quantum-mechanical line-broadening theory like Anderson's[9] may be used to treat the problem, if used in conjunction with Lamb's theory of the laser,[3] but such treatment is outside the scope of this paper. Instead, our concern here will be to give a simple picture pointing out the physical approximations. The task is simplified by the fact that for any reasonable power level, stimulated emission into the cavity mode alone determines the power output of a laser.[10]

Consider an atom in an "inverted state," i.e., entering the higher of the two energy levels involved in the laser action. It will interact coherently with the electromagnetic field present until one of the following happens: (a) it emits a photon; (b) it suffers an inelastic collision [see Eq. (12)]; or (c) it changes its velocity appreciably. First, note that the line-broadening effect due to stimulated emission may be ignored if the laser field is small and only conditions close to the oscillation threshold are considered. However, spontaneous emission of a photon leads to a linewidth, because it interrupts the stimulated emission. This can be calculated using Fourier transformations and sub-

[9] P. W. Anderson, Phys. Rev. 76, 647 (1949).

[10] Apart from terms which are very small in all practical cases.

sequent statistical averages (ensemble average), and it turns out to be Lorentzian with a full width at half-intensity $\delta\omega=2\tau^{-1}$ if the probability of finding the atom in the excited state after a lapse of time t is $\exp(-t/\tau)$. Similar considerations hold for b. (Inelastic collisions cannot usually be described by a single time constant, but the Fourier transform of the interrupted radiation properly averaged still gives a peaked, symmetric line shape.) As for elastic collisions [see Eq. (12)], collisions causing large angular deviations must be treated separately from "soft" collisions of a large impact parameter involving only a small angular deviation of the radiating atom. If in a collision there is a large change in velocity, the corresponding Doppler shift being large, there will be no interaction with the laser field after the collision and stimulated emission is effectively interrupted. On the other hand, if the angular deviation is small and the collision is soft, the atom in question may continue to interact coherently with the laser field. (A collision is considered soft if the phase of the wave function of each atom suffers only small changes during the collision.) The change in velocity, Δv, is large enough to interrupt coherent interaction if $\Delta v/c>1/\omega_0 T_2$, where T_2^{-1} is an effective linewidth determined by $T_2^{-1}=\langle nv\Sigma\rangle_{\Delta v>\Delta v_0}+\tau^{-1}$. The symbol $\langle nv\Sigma\rangle$ denotes a mean collision frequency averaged over those collisions which give a change in velocity Δv larger than a prescribed value Δv_0, where Δv_0 may be determined from

$$\frac{\Delta v_0}{c}\approx\frac{\langle nv\Sigma\rangle_{\Delta v>\Delta v_0}+\tau^{-1}}{\omega_0}. \tag{23}$$

This is an integral equation for the unknown Δv_0 but it can be looked upon as a requirement for the consistency of the picture. If Δv_0 determined from the equation is smaller than the average atomic velocity (in other words, if pressure broadening is smaller than Doppler broadening), the picture is consistent. In the experiment discussed in this paper, a velocity change of 10^3 cm/sec or an angular deviation of about 10^{-2} rad (for an atom of average velocity) is enough to stop stimulated emission. After Δv_0 has been determined consistently, the actual shape of σ can be obtained similarly to cases (a), (b) above.

Two more remarks are in order: First, interaction among atoms causes not only interruption of radiation, but also certain frequency shifts and asymmetries, in principle all calculable, but here introduced phenomenologically. Asymmetry and shift are generally closely related quantities. Second, spontaneous emission and inelastic collisions also determine T_1 in the Boltzmann equation [Eq. (7)], while elastic collisions influence only σ, its magnitude and shape.

The effect of small-angle collisions on the emitted radiation cannot be described by a cross section alone, because during such collisions the phase of the radiating dipole is partly conserved. In other words, when an atom of velocity v disappears because of a small-angle collision, the atom which appears subsequently with velocity $v+\Delta v$ does not start its coherent interaction with the electromagnetic field at a random phase. In the extreme case that Δv is very small,

$$\sigma(v,k,\omega)=\sigma(v+\Delta v,\, k,\, \omega)$$

and the atom continues to emit light at the same rate as before. In a more accurate theory, a density matrix or a dipole moment is the quantity dealt with. These are first-order quantities, and conservation of phase enters the theory naturally. In order to incorporate the effect in the equations of this paper too, note that the Doppler effect is symmetric in v and ω; $\delta\omega=(\mathbf{k}/|k|)\cdot(\omega\mathbf{v}/c)$. Therefore if there is no loss of phase memory during the collision, a change in the velocity of the radiating atom is equivalent to a change in the frequency of the stimulating electromagnetic field. It will in fact be assumed that for such small-angle collisions there is *no* loss of phase upon collision (for discussion, see end of this section). The rest of the calculation is straightforward. Denote the component of atomic velocity along k by $v(t)$; $\omega'(t)=\omega\{1\pm[v(t)/c]\}$ is the effective frequency of the electromagnetic field in a coordinate system moving in the direction of the light with velocity $v(t)$. This frequency-modulated wave can be Fourier analyzed, and the above time dependence of ω' substituted by a statistical distribution of frequencies,

$$P(\omega'')\approx\left\langle\frac{1}{T_2}\int_0^{T_2}\omega'(t)\cos\omega''t\,dt\right\rangle_{\mathrm{Av}};$$

$$\int P(\omega'')\,d\omega''=1. \tag{24}$$

The output power can now be obtained after Eq. (22) is averaged over the above statistical distribution. The width of the distribution function $P(\omega)$ is expected to be proportional to the gas pressure. For simplicity, let us assume a Lorentzian line shape:

$$P(\omega'-\omega)=2s/[s^2+(\omega'-\omega)^2]. \tag{25}$$

This leads to the following expression for the power output:

$$I=\int P(\omega')I(\omega')\,d\omega'$$

$$=K\left\{\frac{G_0-L\exp[+(\omega-\omega_0)^2/2\Delta\omega^2]}{1+\{\gamma\gamma'/[\gamma'^2+(\omega-\omega_0)^2]\}}\right\}, \tag{26}$$

where

$$\gamma=T_2^{-1},\quad \gamma'=T_2^{-1}+s. \tag{27}$$

Thus it is seen that the extent of excessive saturation on exact resonance decreases, and the width of the dip broadens in analogy to inhomogeneous broadening of a resonance line. The additional linewidth s is the reciprocal of a "soft" collision time, $s=1/T_2'$.

Finally the phase shift of the radiating dipole will be estimated in a collision involving a small angular deviation. An inverse power interatomic potential is assumed, $V=V_0+Ar^{-n}$, where V_0 is the unperturbed energy of the level, and r is the distance between the radiating and the perturbing atom. For large n, approximate integration gives for the angular deviation $\Delta\alpha$

$$\Delta\alpha\approx(nA/mv^2)b^{-n}, \tag{28}$$

where b is the distance of closest approach and m and v are the mass and velocity, respectively, in the center-of-mass system. It is assumed that a momentary radiation frequency can be defined, deviating from the unperturbed frequency by

$$\hbar\omega=\Delta V_1-\Delta V_2, \tag{29}$$

V_1, V_2 being the energies of the upper and lower levels of the transition, respectively. It will also be assumed that ΔV_2 is proportional to ΔV_1 which leads to

$$\Delta V_1-\Delta V_2=k\Delta V_1. \tag{30}$$

The total phase shift on collision can be evaluated approximately,

$$\Delta\varphi\approx(kAb^{-n}/\hbar)(b/v) \tag{31}$$

and the ratio of phase shift to deviation angle is

$$\Delta\varphi/\Delta\alpha=bkmv/\hbar n=L(k/n), \tag{32}$$

where $L=mvb/h$ is the relative angular momentum of the collision in units of h.

The assumption of no phase shift for a small-angle collision is good if $\Delta\varphi\ll1$ for a collision with $\Delta\alpha<(\Delta\omega T_2)^{-1}$. The quantities involved are calculable from first principles, but let us test the experimental parameters as obtained in the last chapter of this paper by using them in (33) to obtain $\Delta\varphi$. In effect, the cross section for hard collisions is $\Sigma=\pi b^2$; therefore the formula to be used is

$$\Delta\varphi=\left(\frac{\Sigma}{\pi}\right)^{1/2}\frac{kmv}{\hbar n}\frac{1}{\Delta\omega T_2}.$$

Using the value of b obtained from our measured cross section for He–Ne* collision, we obtain an average value of $L=20$. Assuming that for this collision $K=10^{-1}$, $n=5$, we obtain $\Delta\varphi\ll1$, hence the approximation is valid. On the other hand, for collisions between a Ne atom in the ground state and in a $2s_2$ level (radiatively connected to the ground state), we obtain $L=400$. Assuming now that $n=3$, and k is comparable to unity, $\Delta\varphi$ becomes of the order of unity for $\Delta\alpha=10^{-2}$. For this case, the approximation of small $\Delta\varphi$ is not quite valid.

C. Asymmetric Line Shapes

Explicit use was made of the symmetric shape of $\sigma(v,k,\omega)$ in Eq. (17) and thereafter. It is well known from experiments on pressure broadening that atomic line shapes are usually asymmetric functions of $\omega-\omega_0$. Specifically the ensemble average of the frequency response of atoms with velocity v will now be assumed to be asymmetrical because of pressure effects. In this section, the consequences of asymmetry in σ are explored in the framework of Eq. (14) in the running-wave case, and Eq. (21) in the standing-wave case. The problem is merely that of integration of these equations for a generic asymmetric line shape. Here, as in Sec. 4B, an additional distribution of frequencies smears out the result.

In the running-wave case the result is a shift in frequency of the maximum gain. This is very similar to the shift in the peak of the Doppler broadened line in emission or absorption spectroscopy. Referring to Eq. (14) for a running wave, the integral

$$G=\int n_0(v)\sigma(v,k,\omega)\,dv$$

can be evaluated for a line shape

$$\sigma(v,k,\omega)=\left[\frac{1+\alpha(\omega-\omega_0)}{\gamma^2+(\omega-\omega_0)^2}\right]\sigma_0. \tag{33}$$

This line shape is assumed merely as an example for an asymmetrical average response of an individual atom. This is done in order to examine the influence of slight distortion; (small α), on the over-all Doppler response. For this we obtain

$$G=\sigma_0\frac{(2\pi)^{1/2}}{\gamma}\frac{n}{u}\exp\left[-\frac{(\omega-\omega_0)^2}{2\Delta\omega^2}\right]\times\left[1+\frac{2\gamma\alpha}{2\pi}\int_0^{(\omega-\omega_0)/2\Delta\omega}e^{x^2}\,dx\right]. \tag{34}$$

This has a maximum at approximately

$$\omega=\omega_0+\alpha\gamma(2/\pi)^{1/2}\Delta\omega. \tag{35}$$

This result has to be compared to the value of ω for which σ has its maximum,

$$\omega=\omega_0+\tfrac{1}{2}\alpha\gamma^2. \tag{36}$$

Thus the maximum of a Doppler-broadened line is shifted considerably more than the shift of the response of the individual atom because of asymmetry. The emission of a low-gain running-wave laser is shifted by an amount similar to this, as the term quadratic in σ has a frequency dependence similar to that of the term discussed above.

In the standing-wave case, the relevant equation is Eq. (21). Here both the linear and the quadratic terms have to be considered. In the right-hand side of Eq. (21), the saturated gain can be written after some rearrange-

ment as

$$G(\Delta)=\frac{2}{k}\int n_0\left(\frac{x-\Delta}{k}\right)f(x)\,dx-\frac{2}{k}T_1E^2\Big[\int n_0\left(\frac{x-\Delta}{k}\right)\times f^2(x)\,dx+\int n_0\left(\frac{x}{k}\right)f(\Delta+x)f(\Delta-x)\,dx\Big], \quad (37)$$

where $k=\omega_0/c$, $\Delta=\omega_0-\omega$, and x is a frequency variable. The function f is connected to the cross section σ by the relations

$$f(\Delta-kv)=\sigma(v,k,\omega); \quad f(\Delta+kv)=\sigma(v,-k,\omega). \quad (38)$$

For a frequency deviation $\Delta\ll\Delta\omega$ the integrand can be expanded around $\Delta=0$. Keeping in mind a small but generic asymmetry, $f(x)$ can be divided into a symmetric and purely asymmetric part, the origin being chosen in such a way that the maximum (modal) value of $f(x)$ is at $x=0$.

$$\begin{aligned} &S(x)=1/2[f(x)+f(-x)],\\ &A(x)=1/2[f(x)-f(-x)];\\ &A(0)=A'(0)=A''(0)=0, \end{aligned} \quad (39)$$

where primed and double primed symbols represent first and second derivatives. By a straightforward calculation one finds that the first integral in (31) has a maximum at $\Delta=\Delta^{(1)}$:

$$\Delta^{(1)}=k\frac{\int A(x)n_0'\left(-\frac{x}{k}\right)dx}{-\int S(x)n_0''\left(-\frac{x}{k}\right)dx}, \quad (40)$$

and its frequency response has a width $\Delta\omega$. The rapidly varying part, the third integral in (31), has its maximum at $\Delta^{(2)}$.

$$\Delta^{(2)}=\int S(x)A'(x)\,dx\Big/-\int S(x)S''(x)\,dx. \quad (41)$$

Assuming that the functions n_0 and S differ only to the extent of their characteristic width parameter, the ratio of the line shifts is estimated to be of the order

$$\Delta^{(1)}/\Delta^{(2)}\approx\Delta\omega/\gamma. \quad (42)$$

This leads to a conclusion similar to that in the running wave case. More specifically, the integrals (41) and (42) can be evaluated for the line shape (34), and the result is

$$\Delta^{(1)}\approx\alpha\gamma(2/\pi)^{1/2}\Delta\omega, \quad (43)$$

$$\Delta^{(2)}\approx\alpha\gamma^2. \quad (44)$$

This is similar to (36) and (37), i.e., the "center of the dip" moves by a small amount only, while the maximum of the unsaturated gain is displaced by a fraction which is $\Delta\omega/\gamma$ larger. It can also be shown that for a small asymmetry, $\alpha\gamma\ll1$, The shape of the quadratic term is quite symmetric. Thus in a standing-wave laser in the presence of an asymmetric line broadening the output power, Eq. (27), has to be modified to

$$I(\omega)=K\left\{\frac{G_0-L\exp[+(\omega-\omega_0-\Delta^{(1)})^2/2\Delta\omega^2]^2}{1+\gamma\gamma'/[\gamma'^2+(\omega-\omega_0)^2]}\right\}. \quad (45)$$

This is the equation used to fit the experimental points, the five free parameters to be varied by the computer being $K/L=A$; $G_0/L=B$; $\gamma'/\Delta\omega\sqrt{2}=C$; $\gamma/\gamma'=D$; $-\Delta^{(1)}/\Delta\omega\sqrt{2}=E$.

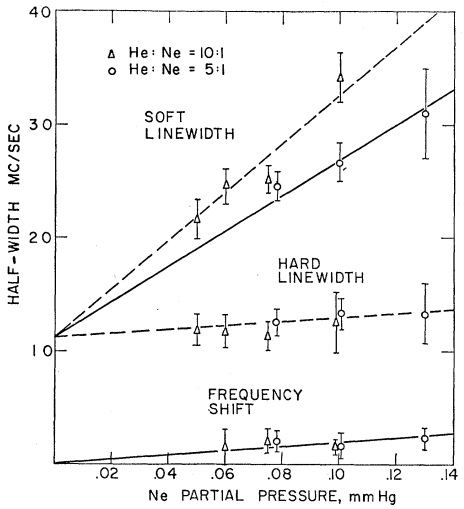

FIG. 4. Experimental results for linewidths and asymmetries of the Ne transition.

5. RESULTS AND INTERPRETATION

It was found that Eq. (45) describes experimental results to within the expected accuracy. Experiments were carried out with two different gas mixtures, He:Ne=10:1, 5:1 and in the pressure ranges He: 0.4–1.0 Torr and Ne: 0.05–0.13 Torr. Results are summarized in Fig. 4. Vertical bars denote standard deviations, the actual fit of the experimental points to the straight lines being much better.

Pressure broadening of the line, as described by parameters γ, γ', can be accounted for by collisions of the radiating atoms with other atoms in the gas. The general formula is[11]

$$\begin{aligned} \gamma&=\gamma_N+\Sigma_{\mathrm{Ne}}\bar{v}_{\mathrm{Ne-He}}n_{\mathrm{Ne}}+\Sigma_{\mathrm{He}}\bar{v}_{\mathrm{Ne-He}}n_{\mathrm{He}},\\ \gamma'&=\gamma+\Sigma_{\mathrm{Ne}}'\bar{v}_{\mathrm{Ne-Ne}}n_{\mathrm{Ne}}+\Sigma_{\mathrm{He}}'\bar{v}_{\mathrm{Ne-He}}n_{\mathrm{He}}. \end{aligned} \quad (46)$$

Here γ_N is the contribution due to the natural lifetime of the upper excited level $2p^5(^2P_{1/2}{}^0)4s(J=1)$, $\bar{v}_{\mathrm{Ne-Ne}}$

[11] A. C. G. Mitchell and M. W. Zemansky, *Resonance Radiation and Excited Atoms* (MacMillan and Company, Ltd., London, 1934), p. 170.

and $\bar{v}_{Ne-He}$ are the mean relative velocities of the atoms, and n_{Ne}, n_{He} are their concentrations. Four types of collisions have been taken into account: collisions of the excited Ne atom with a ground state Ne atom—this can be "hard" Σ_{Ne-Ne} or "soft" Σ_{Ne-Ne}' and collisions of the excited Ne atom with a ground-state He atom, Σ_{Ne-He} and Σ_{Ne-He}' respectively. The results are

$$\begin{aligned}\Sigma_{Ne-Ne}&=1.6\times10^{-14}\text{ cm}^2,\\ \Sigma_{Ne-Ne}'&=8\times10^{-14}\text{ cm}^2,\\ \Sigma_{Ne-He}&=5\times10^{-16}\text{ cm}^2,\\ \Sigma_{Ne-He}'&=4.5\times10^{-15}\text{ cm}^2.\end{aligned}\tag{47}$$

These cross sections are of the right order of magnitude. It has to be borne in mind that the upper laser level is radiatively connected to the ground state of Ne, and therefore reabsorption of the uv photon is an important mechanism for energy transfer. A more thorough study of this effect will be given in a forthcoming paper. Collisions with the He atoms are also near-resonant as there is an excited state of He(2^3S) within kT of the Ne state. This may explain the large ratio $\Sigma_{Ne-He}'/\Sigma_{Ne-He}$, which could be expected to be ~2 for a pure dispersion-type force.

The frequency shift is towards higher frequencies in the sense that in Eq. (34) α is positive. Assuming that this shift is proportional to the pressure and using Eqs. (44) and (45), one obtains a shift associated with the response of individual atoms given by

$$\Delta^{(2)}=(\gamma/\Delta\omega)\Delta^{(1)}\cong200\text{ kc/sec Torr}.\tag{48}$$

This estimate can be somewhat too low because the exact ratio of $\Delta^{(2)}/\Delta^{(1)}$ depends critically on the details of the actual asymmetry. Furthermore, it should be noted that the shift as measured in our experiment does not give the absolute shift of the over-all atomic resonance and it is only a measure of that introduced by the asymmetry.

6. CONCLUDING REMARKS

In the past, studies of pressure effects at optical frequencies were limited to high-pressure regions where collisional broadening of a spectral line becomes larger than its Doppler width. With our experimental approach, however, we are able to detect the effects of collisions at much reduced pressures. This has been made possible because our measurements are particularly sensitive to saturation behavior of an atomic transition. This saturation effect, in turn, depends primarily on the average response of individual atoms. Accordingly, we are able to observe the average response of individual atoms at much reduced pressures where the width due to collision is much less than the Doppler width. It should be pointed out that details of collision effects at elevated pressures are theoretically complex and somewhat involved. This is generally the case because at high pressures the contributions of many-body collisions become sizable and effects such as screening of two colliding atoms by other atoms need to be taken into account. Hence, the eventual interpretation of experimental data in terms of the actual interactomic forces may be dealt with more readily once the observations are done at reduced pressures.

It should also be pointed out that in double-resonance or level-crossing experiments, the observed width of a resonance is also associated with the average response of an individual atom. However, a number of interesting pressure effects, such as the influence of asymmetry of the line shape as described in this paper, do not appear directly in double-resonance or level-crossing line shape. These latter experimental techniques also provide useful information. At this time, however, the observed line shape at optical frequencies and at reduced pressures reveal novel features of perhaps new theoretical interest.

An individual atom while interacting with an applied optical field is constantly disturbed by the presence of other atoms. In a detailed theory of pressure effect, an excited atom may not be considered as a freely interacting system during any portion of its lifetime. The object of a theory to explain our present experimental results is not merely to treat the linear response of the atomic resonance. The major goal is actually to deal with the effect of collision on saturation behavior of the Doppler-broadened transition. Furthermore, this needs to be done for an optical field in the form of standing waves. Already, considerable information exists on the general influence of the collision effect on the linear frequency response of an atomic line shape. The point of view and the approach adapted in this paper have been based on utilizing our general knowledge and expectations on the average linear response of individual atoms, and from them to construct a Doppler line shape which includes the saturation term. In this treatment, we have assumed that the ensemble average of the response of individual atoms with a given velocity v is known in the presence of perturbing fields due to interatomic interactions; this average may have an asymmetrical frequency response. The reasons for such an asymmetry are well known. One interesting result which comes out of this treatment is an account of the way in which the asymmetry leads to an observed frequency shift considerably larger than that associated with the shift introduced on the response of an individual atom. In other words, we find that if an average asymmetrical response introduces a shift of the order of $\alpha\gamma^2$, the frequency corresponding to maximum saturation of the over-all Doppler response is shifted roughly by $\alpha\gamma\Delta\omega$. While our treatments adequately account for this effect as well as those collisions which are classified as "hard" collisions, our treatments of "soft" collisions require considerably further refinements.

On the experimental side, it is extremely important to exercise utmost care so that distortions introduced by measuring techniques are kept at a minimum and are fully allowed for in extracting the actual line shape.

In our experiments, we find that the expression (45) fully accounts for frequency behavior of the output power after all instrumental distortions are reduced below our other experimental errors.

These experiments are continuing using other frequency-tuning techniques and applied to other laser transitions.

ACKNOWLEDGMENTS

One of the authors (A. S.) wishes to thank Dr. S. Alexander for his helpful discussions. We would also like to acknowledge the able assistance given by Eugene Leonard and Richard Solomon in the course of this work. The assistance of R. H. Cordover in preparation of this manuscript is also acknowledged. This work was done in part at the MIT Computation Center, Cambridge, Massachusetts.

APPENDIX

In the Appendix a more formal development of the theory will be given. The frequency equation of the laser operation is also derived along the lines of Sec. 4, and it will be shown to be equivalent to Lamb's[3].

The electromagnetic field of the laser cavity is expanded in cavity modes in a one-dimensional standing-wave cavity:

$$\begin{aligned} &E(x,t)=E_n(t)U_n(x),\\ &E_n(t)=E_n^{(0)}\cos\omega_n t,\\ &U_n(x)=\sin k_n x;\quad k_nL=n\pi. \end{aligned} \tag{A1}$$

Maxwell's equations of the cavity in cgs units are

$$(d^2E_n/dt^2)+(\omega_n/Q_n)(dE_n/dt)+\Omega_n^2E_n=4\pi\omega_n^2P_n. \tag{A2}$$

Here $\Omega_n=k_nc$, Q_n is the quality factor of the cavity and P_n is the projection of the macroscopic polarization of the medium on the nth mode. It has in-phase and out-of-phase components,

$$P_n=C_n\cos\omega_n t+S_n\sin\omega_n t. \tag{A3}$$

Substitution in (A2) yields the amplitude and frequency equations

$$dE_n/dt+(\omega_n/2Q_n)E_n=-2\pi\omega_nS_n, \tag{A4}$$

$$(\omega_n-\Omega_n)E_n=-2\pi\omega_nC_n. \tag{A5}$$

The development so far parallels Lamb's the only difference is in the units used. The individual atoms of the amplifying medium are described by a complex electric susceptibility $\chi(\mathbf{v},\mathbf{k},\omega)$. The velocity dependence comes from the Doppler effect, and it is assumed that the electromagnetic field is decomposed into running waves. This susceptibility satisfied the Kramers-Kronig relations, so its imaginary part is in principle calculable from its real part, $\sigma(v,k,\omega)$. For simplicity it will be assumed that σ has a Lorentzian line shape and it is an isolated resonance. Under these assumptions

$$\begin{aligned} \chi(\mathbf{v},\mathbf{k},\omega)&=\sigma_0\left\{1+i\left[\omega-\omega_0\left(1-\frac{\mathbf{k}\cdot\mathbf{v}}{|k|c}\right)\right]T_2\right\}^{-1},\\ &=\sigma(\mathbf{v},\mathbf{k},\omega)+i\rho(\mathbf{v},\mathbf{k},\omega). \end{aligned} \tag{A6}$$

In order to get the susceptibility for the gas as a whole, Eq. (A6) has to be integrated over the velocity distribution:

$$S_n=E_n\int[\sigma(\mathbf{v},k_n,\omega_n)+\sigma(\mathbf{v},-k_n,\omega_n)]n(\mathbf{v})\,d\mathbf{v}, \tag{A7}$$

$$C_n=E_n\int[\rho(\mathbf{v},k_n,\omega_n)+\rho(\mathbf{v},-k_n,\omega_n)]n(\mathbf{v})\,d\mathbf{v}. \tag{A8}$$

It can be seen that with this substitution Eq. (A4) reduces to Eq. (6) in the text. In order to find $n(v)$ a Boltzmann equation, Eq. (7) will be used, and in particular Eq. (19):

$$\begin{aligned} n(v)=\frac{n}{u(2\pi)^{1/2}}\exp\left[-\frac{(\omega-\omega_0)^2}{2\Delta\omega^2}\right]\{1-T_1'E^2(k,\omega)\\ \times[\sigma(v,k,\omega)+\sigma(v,-k,\omega)]\}. \end{aligned} \tag{A9}$$

The expressions for S_n may now be obtained by using the above equation in (A7). The resulting expression in conjunction with (A4) gives a result identical to our Eq. (22) for $L=\omega_n/2Q$. The expression for C_n may be estimated similarly by integrating (A8) using (A9). This expression will not be given here since the result is exactly identical to that estimated by Lamb.

In terms of C_n and S_n, the frequency equations in the steady state can be written in the form

$$[(\omega_n-\Omega_n)/\omega_n]2Q_n=C_n/S_n. \tag{A10}$$